Experimental Investigation of Pool Boiling Heat Transfer and Critical Heat Flux on a Downward Facing Surface

M. Gocmanac[1] and J. C. Luxat[2]
[1]AMEC-NSS, Toronto, Ontario, Canada
[2]McMaster University, Hamilton, Ontario, Canada
(luxatj@mcmaster.ca)

Abstract

A separate effects experimental study of heat transfer and Critical Heat Flux (CHF) on a downward facing plate in subcooled water pool boiling is described. Two geometries of downwards facing surfaces are studied. The first is termed the 'confined' study in which bubble motion is restricted to the heated surface. The second is termed the 'unconfined' study where individual bubbles are free to move along the heated surface and vent in any direction. The method used in the confined study is novel and involves the placement of a lip surrounding the heated surface. The CHF as a function of angle of inclination of the surface is presented and is in good agreement with other experimental data from somewhat different test geometries.

1. Introduction

Severe accidents in nuclear reactors are generally defined as accidents involving damage to fuel or structures within the reactor core (core degradation) due to sustained inadequate heat removal from the fuel. Severe accident research and analysis became an area of significant focus following the Three Mile Island Unit 2 and Chernobyl Unit 4 accidents in 1979 and 1986, respectively and no doubt will be of continued focus following the 2011 events at Fukushima Daiichi. Severe accidents are particularly challenging in that they bring into play many phenomena that impose extreme challenges to the integrity of internal plant structures and containment itself. At the same time the thermal-chemical-mechanical phenomena accompanying core degradation are also very difficult to characterize through both experimental and analytical means normally employed in nuclear safety analysis.

CANDU reactors have a number of heat sinks that can either delay or limit the progression of a severe accident. However, severe accidents cannot be precluded. An example of an event sequence that results in a particularly challenging severe accident is a station blackout leading to a sustained loss of all heat sinks. In such an event significant damage to the reactor will occur such that fuel channels disassemble (collapse) resulting in the formation of a debris bed at the bottom of the calandria vessel. Continued heatup of the debris bed will lead to formation of a molten corium pool (corium is a mixture of the uranium-zirconium-oxygen material from the fuel and fuel channels), which is likely to be contained in a solid crucible formed at the bottom of the calandria vessel and at the top of the molten corium pool. At the top of the corium pool most of the heat is transferred by radiation to the cooled walls of the calandria vessel. At the bottom of the pool a quasi-equilibrium state is reached where downwardly directed convected heat is transferred by conduction through the calandria vessel wall to the shield tank water outside the calandria vessel. Progression of such severe accidents in CANDU reactors has been studied and reported in the open literature [1,2,3].

One possible mode of calandria vessel failure is due to creep deformation if the wall temperature becomes sufficiently high that the steel vessel wall loses strength and strains to failure [4] . For the temperature of the calandria vessel wall to remain sufficiently low such that creep deformation does not occur it is necessary that Critical Heat Flux (CHF) not occur on the outside of the vessel wall where heat is being transferred from the melt pool. This requires that there be confidence, supported by experimental data regarding the limiting value of CHF for downward facing surfaces since the ability to remove heat by boiling heat transfer depends upon the ability to vent any vapour that forms on the lower portions of the wall. If vapor cannot be removed from local regions of the wall then sustained film boiling is likely, with a related significant increase in wall temperature.

The experiments discussed here are designed to measure the CHF as a function of the angle of inclination of a downward facing heated surface under situations where vapour transport from the heated surface is either obstructed or unobstructed. Obstructions to venting could exist in the region of the moderator outlet flow nozzles. The heated surface is representative of local sections of the vessel wall. Therefore, the experimental data are of direct relevance to the issue of in-vessel retention of molten corium in a CANDU reactor.

2. Pool Boiling Heat Transfer

Although pool boiling is a well researched area there is still a lack of complete understanding of many aspects, especially for downward facing heated surfaces. For example, there is debate on whether the vapour bubbles are formed directly on the heated surface or in a superheated liquid layer adjacent to the heated surface [5]. Water purity and heater surface oxidation are known to affect boiling and CHF [6] although the effects are not fully characterized. A number of published experimental studies have been reported in the literature [7,8,9,10] and the measured values of CHF in these experiments vary, ranging from ~200 kW/m^2 [8] to ~700 kW/m^2 [10].

There is a lack of data for downwards facing orientations and even further lack of data for confined boiling. One group of researchers recently derived a correlation for boiling heat transfer on a downward facing heated surface in pool boiling under confined conditions [11]. This study unfortunately did not measure CHF, and focused solely on characterizing pre-CHF boiling. Part of the motivation for the experiments reported here is to attempt a novel confinement of vapour bubbles on the heated surface and evaluate the effect of the confinement on the heat transfer.

3. Experimental Apparatus

The key component of the experimental apparatus employed is the heated element. Two designs of the heated element were constructed, denoted as the “confined” and “unconfined” heated elements. The confined design restricts vapour bubble motion to the centre disk of the heated element. In the unconfined design, once a bubble nucleates it is free to move along the entire heated element in any direction. The two designs are shown in Figure and Figure 2, respectively. The figures show the top view of the heated element in the centre along with three section views.

The confined design of the heated element is composed of a brass cylinder containing 28 cartridge heaters, 12 thermocouples, a Mullite tube, flexible ceramic fibre blanket, and an aluminum shell. Silicone is used as an adhesive and sealant between the brass cylinder and Mullite tube and the Mullite tube and aluminum shell. The lip height in the confined design is approximately 4 mm. In the unconfined design, the Mullite tube is eliminated and the bottom of the brass cylinder is made flush with the bottom of the Aluminum shell. Silicone is applied between the Brass rod and the Aluminum shell only.

The brass cylinder, 86.4 mm in diameter and 101.6 mm in length consisting of free machining brass (360 brass), is precision machined to allow for the insertion of the cartridge heaters, thermocouples and a threaded support rod. Four sets of seven cartridge heater holes arranged in a honeycomb pattern are drilled and then reamed to a diameter of 9.525 mm ad a depth of approximately 50.8 mm. To optimize heat transfer from the heaters to the brass cylinder a thermally conductive liquid is applied to the Inconel sheath before the cartridge heaters are inserted into their respective holes. Each cartridge heater generates a maximum power of 350 W at 100 VDC. The maximum instantaneous power that can be input into the heated element is therefore 9.8 kW.

Two sets of six thermocouple access holes with a diameter of 4 mm and tight tolerances on depth are arranged radially in the brass cylinder. The thermocouple access holes have two different depths (Section Views B-B and C-C of Figures 1 and 2). To ensure good tip contact ceramic cement is applied to the sides of the thermocouple sheath before the thermocouples are inserted into their respective access holes. Type K grounded junction thermocouples with OD of 3.175 mm are inserted in the thermocouple access holes in the brass cylinder.

A threaded rod is inserted in the top centre of the heated element to provide structural support. The rod is made of galvanized carbon steel. A ceramic fibre blanket is used to thermally insulate the top and sides of the brass cylinder The ceramic fibre blanket is inserted as part of the assembly after the aluminum shell has been joined to the element by the silicone adhesive. An aluminum shell bonded to the brass cylinder (unconfined design) or the Mullite tube (confined design) is used to prevent the ceramic fibre blanket from absorbing water. The Mullite tube has an ID of 86.87 mm and a wall thickness of 9.525 mm.

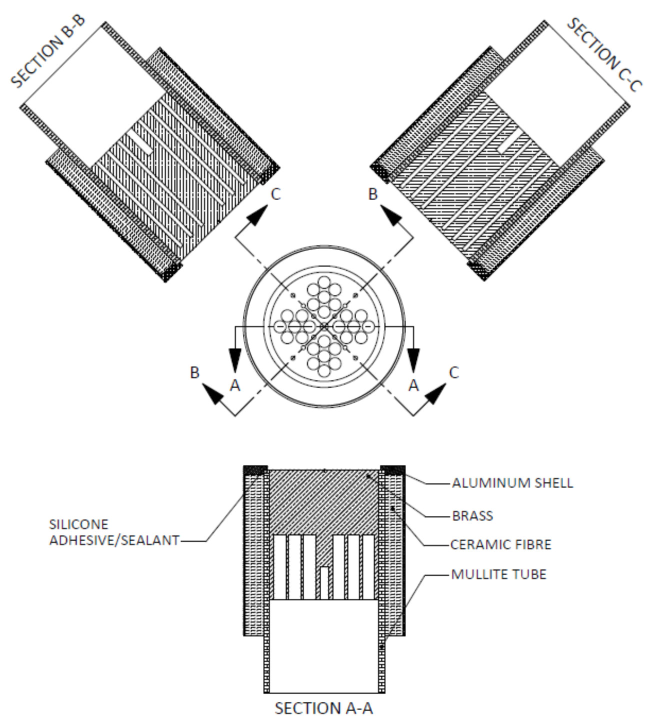

Figure 1: Confined Design

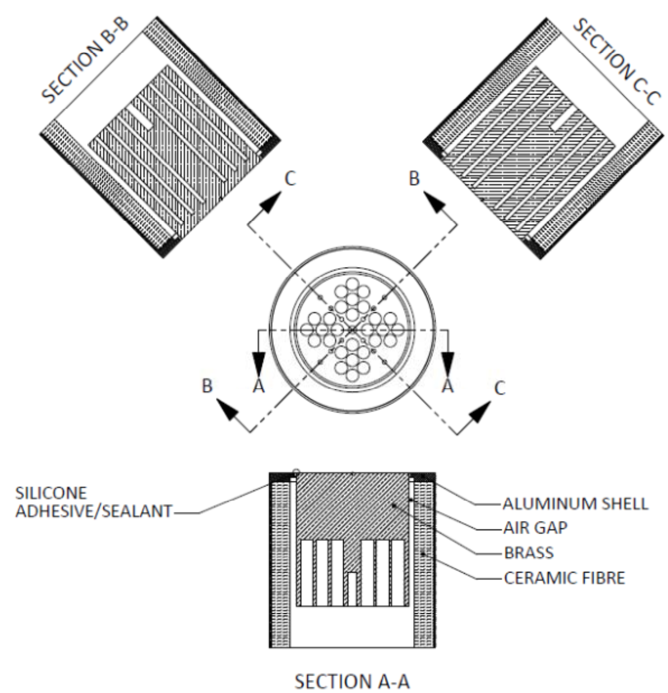

Figure 2:Unconfined Design

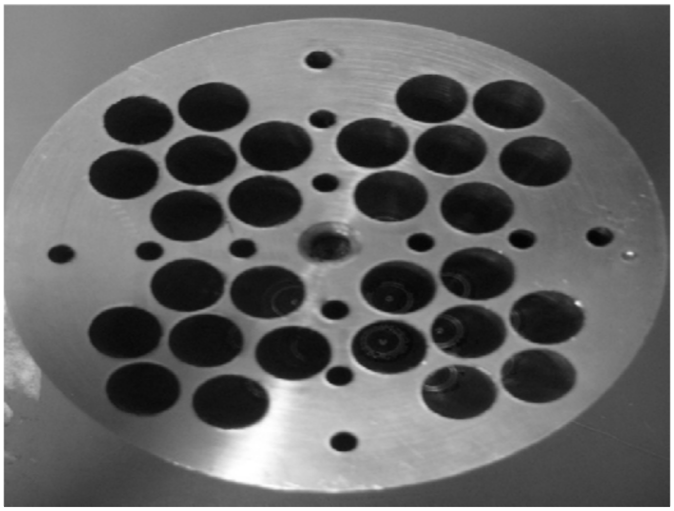

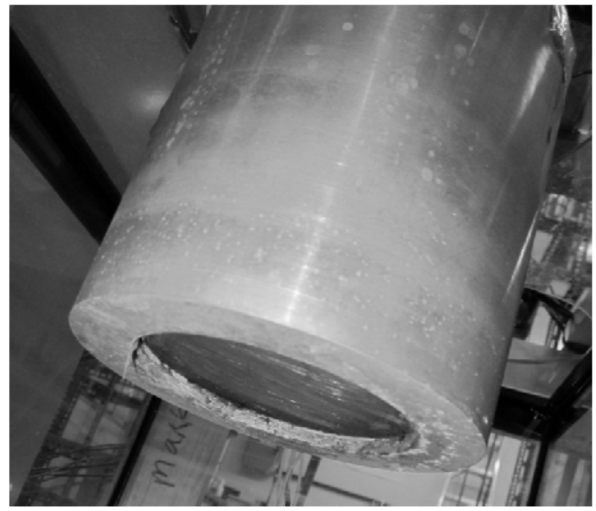

Figure 3: Top View of Brass Cylinder **Figure 4: Confined Design End View**

A top view of the precision machined brass cylinder is shown in Figure 3 and the bottom end view of the confined design is shown in Figure 4. The heated element is submerged in a pool of water to a sufficient depth such that any waves generated by boiling on the downward facing surface do not strongly influence the thermal-hydraulic behaviour at the heater-water interface. A 25 mm depth of submergence was found to be adequate.

The threaded rod provides structural support in both the confined and unconfined heated element designs and the upper end of the rod is attached to an aluminum disk that is supported by two carbon steel rods attached to two flat bars that are part of the main chassis. Adjustment of the angle inclination of the heated element is achieved by changing the holes that the carbon steel rods penetrate on the main chassis. An isometric assembly of the components needed for angle adjustment is shown in Figure 5.

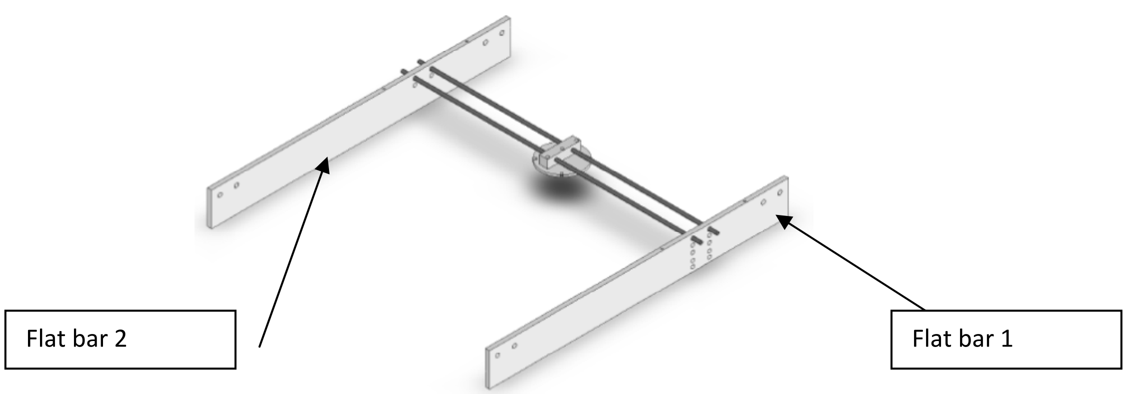

Figure 5: Angle Adjustment (Showing 0° Inclination)

Directed heat flux from the bottom of the heated element is obtained by insulating all sides except the bottom surface. The maximum temperatures in the device are required to be estimated in order to ensure that the selected materials are not taken beyond their limits. Based upon prevention of melting of the brass cylinder at the top surface a power limit for this heated element design as being 6.5 kW. The cartridge heaters are arranged in a way to minimize the variability in temperature along the exposed surface. The goal is to have a temperature distribution that peaks not at the geometric centre line of the brass cylinder but instead somewhere between the geometric centre line and edge. The thermal conductivity of the element is the strongest parameter affecting the temperature gradient along the surface and axially. The maximum variation from the mean is approximately 2 ˚C, as shown in Figure 6.

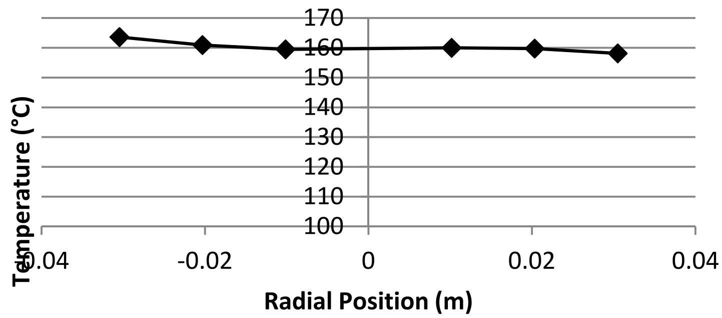

Figure 6. Radial Temperature Variability along Bottom Surface of Heated Element: Unconfined Design

4. Test Matrix

For the unconfined heated element design only one experiment is performed. The device is oriented downwards with a 0˚ inclination and the temperature of the bulk is maintained at nominally 35 ˚C.

The confined design was studied in 15 different experiments. The angle of inclination and bulk fluid temperature is varied between the allowable ranges established in the test matrix, shown in Table 1.

Table 1: Test Matrix for Confined Design

T_{∞} □	0°	2.5°	5°	6°	20°
25°C	X	X			
30°C	X	X	X	X	X
35°C	X	X	X	X	X
40°C			X	X	X

An 'X' indicates that the test was performed successfully for the conditions shown. For the 0˚ and 2.5˚ inclination it was not possible to maintain T_∞ at 40 ˚C. For 5˚, 6˚, and 20˚ an experiment with T_∞ at 25 ˚C was not attempted.

5. Heat Flux Determination

The heat flux through the exposed surface is calculated from the measured temperature values. The heat flux through the unheated portion of the Brass cylinder is linear axially. To determine the downwards heat flux:

$$q = k\frac{T_2 - T_1}{\Delta y} \qquad (1)$$

Where:

T_2 is the average of the temperatures values of thermocouples located in the upper section of the heated element.
T_1 is the average of the temperatures values of thermocouples located in the lowerr section of the heated element.
Δy is the difference in depth between the two thermocouple levels, and
k is the thermal conductivity of the Brass cylinder.

In the calculation of the heat flux, no temperature values were discarded as outliers. All temperature values are used. The separation distance, Δy, is fixed and is set by the differing hole depths. The thermal conductivity, k, is a function of temperature and is evaluated at the mean temperature of all heated element temperature recordings. The thermal conductivity is evaluated with only one input: $T_{1,2} = \langle T_2, T_1 \rangle$, where T is in Kelvin. The expression for k is:

$$k(T_{1,2}) = a + b(T_{1,2} - 273) \qquad (2)$$

Where a and b are calculated as 75.82 $Wm^{-1}K^{-2}$ and 0.1183 $Wm^{-1}K^{-2}$ [12] .

The heat flux is calculated using Equation 1 for all available data. However, in construction of the boiling curve only steady state data is used. The approach used is to calculate an average heat flux from the last 50 data points. An alternative approach would be to calculate the heat flux at the very last available data point. Both approaches yield similar results, but the former approach facilitates statistical analysis of the data. The following table summarizes the individual values in Equation 3.1 for a heat flux of ~500 kW/m^2. The surface temperature was not directly measured, but was evaluated by linear extrapolation from the measured temperature values. The following expression is used to find the surface temperature:

$$T_w = T_1 - \frac{1}{2}(T_2 - T_1) \qquad (3)$$

The above expression is a special case of linear extrapolation and is valid because the distance between the surface and the first set of thermocouples is 2.54 mm, which is precisely half of the separation distance.

Table 2: Values of Parameters in Equation 1

Parameter	Numerical Value
k	127 W/mK
ΔT	20 ˚C
Δy	5.08 mm

A boiling curve is constructed for each experiment. Upon departure from nucleate boiling the temperature of the heated element rises rapidly and in some cases non-uniformly. Calculating the CHF as the temperature of the heated element is rapidly increasing is not practical and is prone to large errors. The approach was to determine the CHF by linear extrapolation from the known nucleate boiling data point. The heat flux extrapolation is based on the measured power level that resulted in film boiling, i.e.:

$$q_{CHF} = \frac{p_{CHF}}{p_{NB}} q_{NB} \quad (4)$$

Where the subscript *NB* refers to the last known nucleate boiling data point, p_{NB} is the power level at the last nucleate boiling point and p_{CHF} is the power level at departure from nucleate boiling.

Once the power level is increased the temperatures can exist in a quasi-steady state for a significant period of time before film boiling is instigated. For these cases it is possible to compare the result calculated by equation 3.4 with the measured heat flux just before the temperature excursion occurred. The values are found to match almost exactly. The following systematic errors were identified and evaluated:

- Thermocouple accuracy
- Manufacturing tolerances in hole depth
- Differing rates of thermal expansion
- Recirculation system impact on thermal-hydraulic behaviour
- Pool temperature thermocouple impact on thermal-hydraulic behaviour
- Wear and aging of the heated element
- Level fluctuation in test section tank
- Thermocouple drift or fouling
- Quantization error

6. Experimental Results

6.1 Confined Study - Boiling Curve

The heat flux through the exposed surface is plotted as a function of wall superheat, ΔT, for the confined design in Figures 7 through 11. An abrupt transition from nucleate boiling to film boiling was observed in the confined design. The resulting temperature excursion would lead to temperature measurements in excess of 200 ˚C. Also, the individual temperature measurements would increase by 50 ˚C or more compared to the nucleate boiling value. Power is removed as soon as the temperature recording approaches 200 ˚C. CHF was not reached for the 20˚ inclination to avoid potential damage to the heated element. The CHF value for this angle of inclination is extrapolated from the boiling curve data as follows: 200 ˚C is divided by the peak temperature observed and is used to multiply the heat flux at the peak power. Thus, this calculation is intended to show that the CHF is monotonically increasing as inclination angle is increased. The measured CHF as a function of inclination angle is plotted in Figure 12 and a comparison with published data for a sallow curved downward facing surface is given in Figure 13. Note that the data shows little spread in CHF values for different pool temperatures. Table 3 presents the values of CHF for a pool temperature of 30 ˚C.

Table 3: CHF Table of Values for T_∞=30 ˚C

Theta	CHF (kW/m^2)
20	596
6	495
5	295
2.5	223
0	187

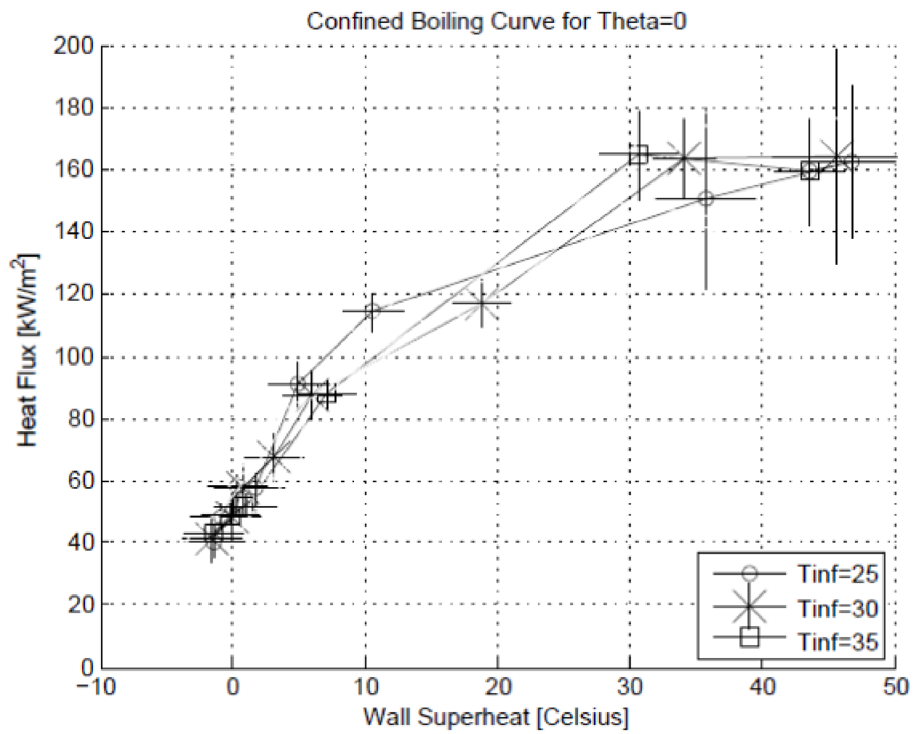

Figure 7: Boiling Curve, Confined Design, θ=0°

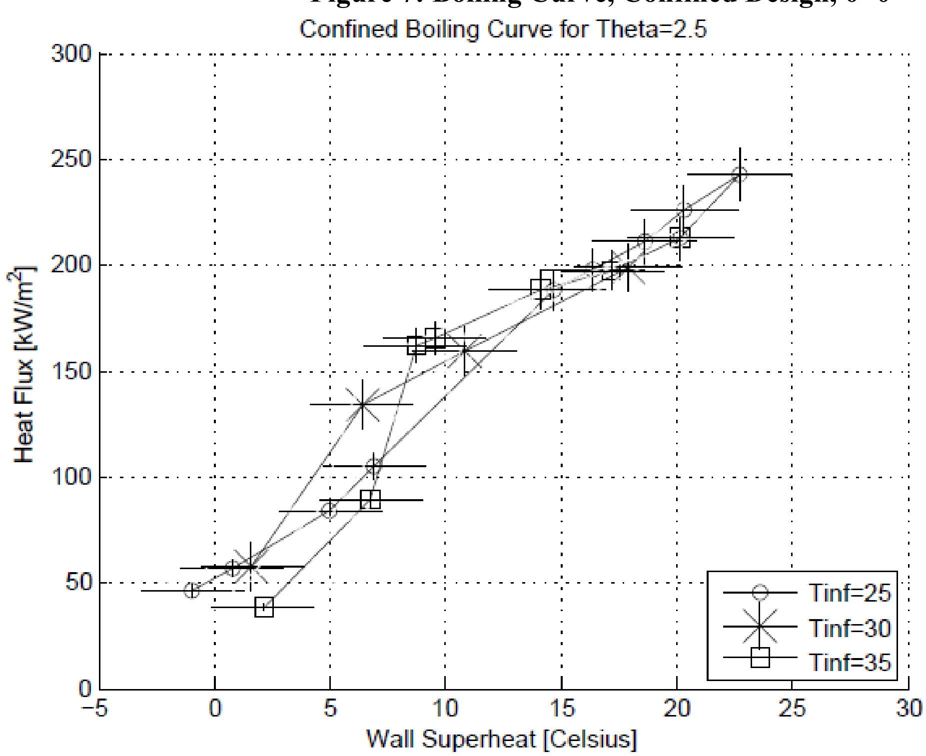

Figure 8: Boiling Curve, Confined Design, θ=2.5°

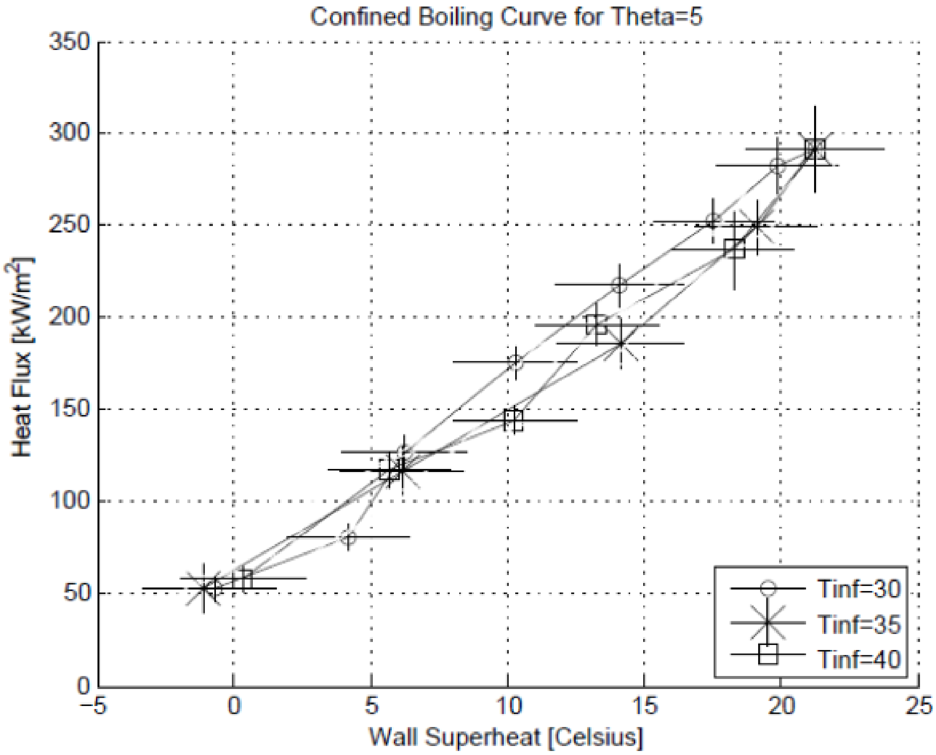

Figure 9: Boiling Curve, Confined Design, θ=5°

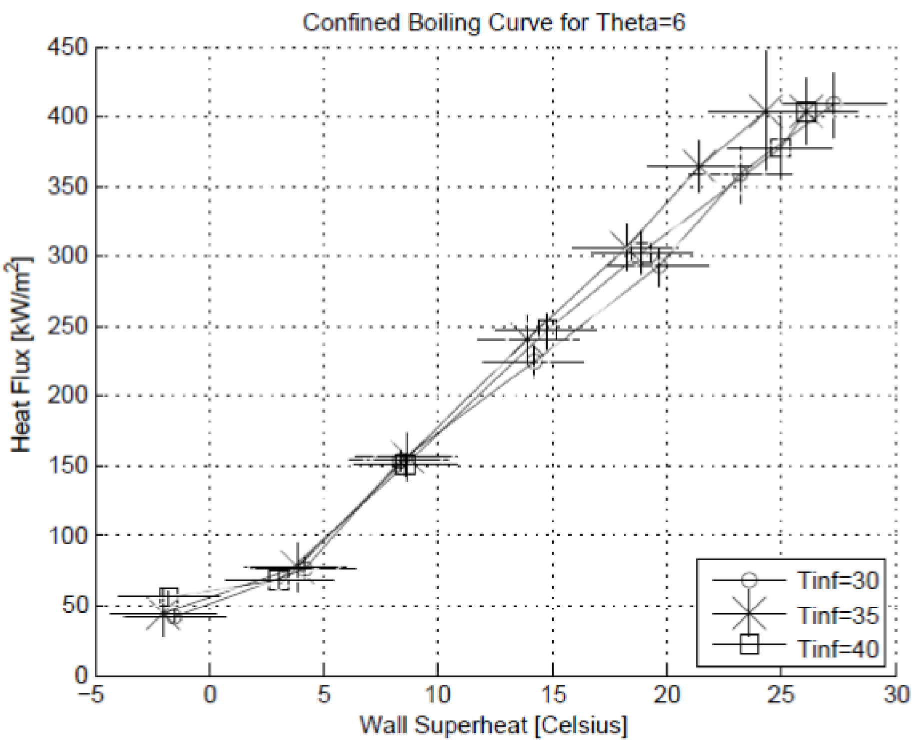

Figure 10: Boiling Curve, Confined Design, θ=6°

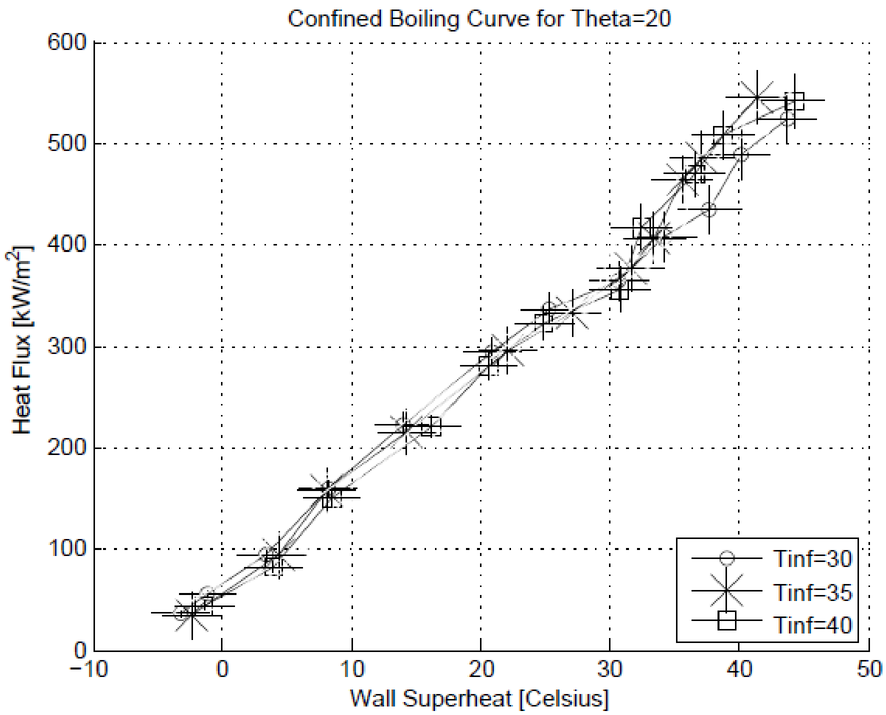

Figure 11: Boiling Curve, Confined Design, θ=20˚

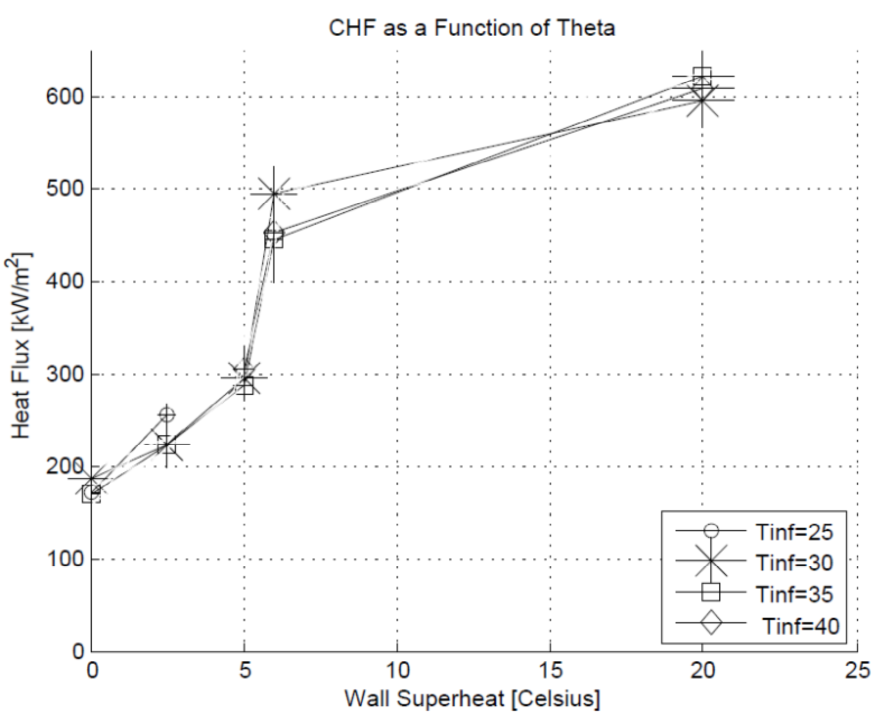

Figure 12: CHF as a Function of θ

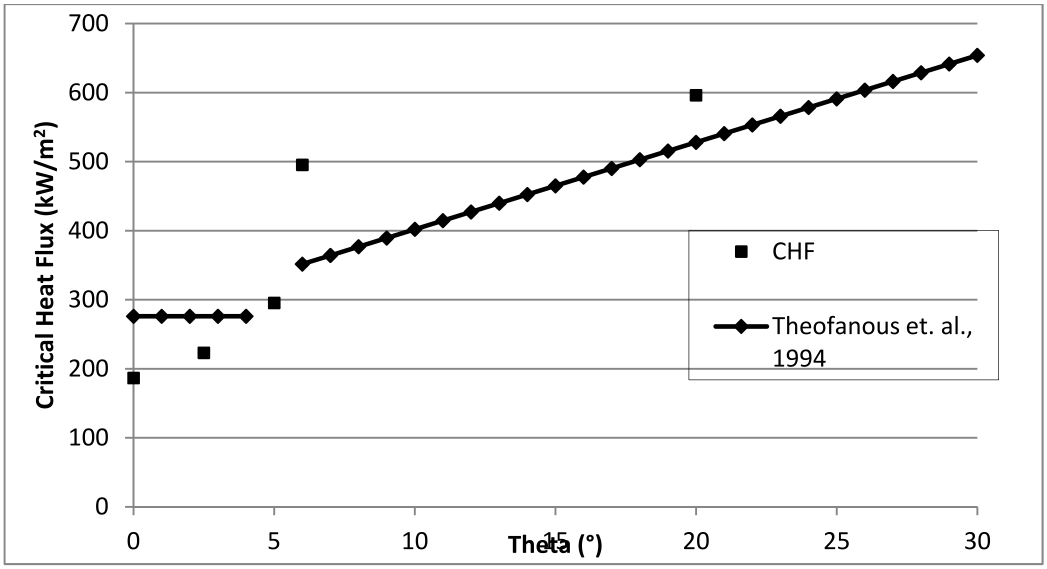

Figure 13: CHF as a function of θ – Comparison with Theofanous data

6.2 Unconfined Study - Boiling Curve

The heat flux through the exposed surface is plotted as a function of wall superheat, ΔT, for the unconfined design in Figure 14.

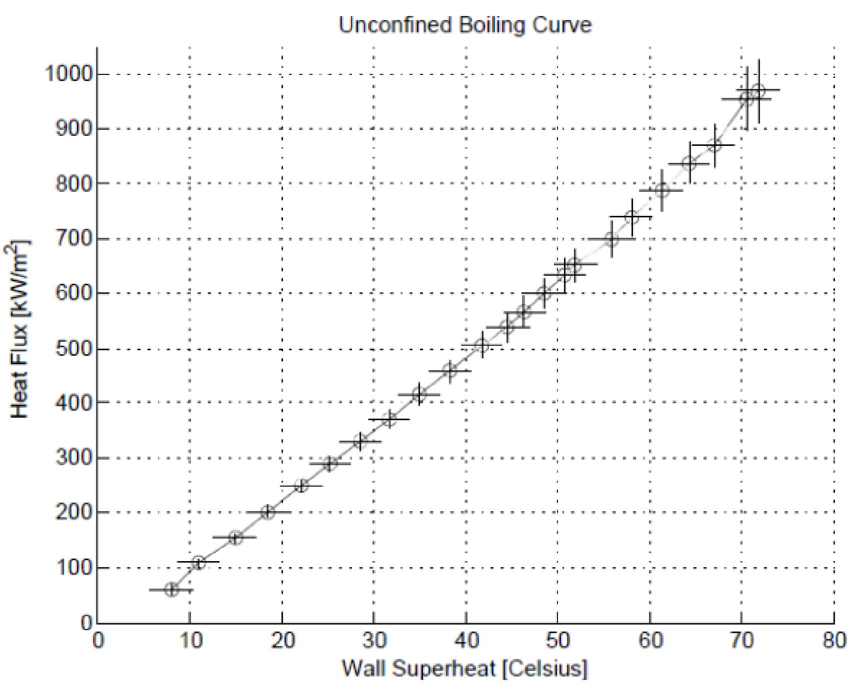

Figure 14: Boiling Curve, Unconfined Design

The lowest power occurrence at which transition from nucleate boiling to film boiling occurs is defined as the CHF. For the unconfined design, it is expected that a temperature excursion would result or that the wall temperature would rise above 200 ˚C. This transition was not observed experimentally in these tests since the CHF for this geometry is greater than ~1 MW/m^2, a heat flux which could lead to heater element failure due to melting at the upper surface of the brass cylinder.

7. Conclusions

A successful experimental investigation of boiling heat transfer and crtitical heat flux on downward facing surfaces in pool boiling has been conducted. A novel confinement technique was employed using a lip arrangement around the edge of the heated surface. The extent of confinement was adjusted by varying the inclination angle for a surface in which venting was obstructed by the lip surrounding the heated surface. This arrangement also allowed for separation of the effects of condensation and venting as a method of heat removal. The CHF results as a function of inclination angle were compared to data obtained by Theofanous et al [7] and good agreement was observed, particularly for the inclination angle of 5.5^o at which a step increase in CHF occurs due to enhanced steam venting. Similar results were also obtained with regards to an observed transition angle in the CHF-Angle of Inclination plot. The critical angle that allowed for venting was $\theta=2.5°$ with CHF increasing as the angle of inclination is increased.

The unconfined heated element design never attained CHF because of limitations on power and concern with melting of the upper portion of the heated element. However, it is concluded that for the unconfined geometry CHF is greater than 1 MW/m^2. The effect of size of the surface (scale effect) on this result is under investigation.

8. Acknowledgements

The financial support of the Natural Sciences and Engineering Research Council (NSERC) and the University Network of Excellence in Nuclear Engineering (UNENE) is gratefully acknowledged.

9. References

[1] J.C.Luxat (2009), “Thermalhydraulic Aspects of Progression to Severe Accidents in CANDU Reactors”, *Nuclear Technology* , Vol. 167, No. 1, pp 187-210.
[2] Dupleac, D., Mladin, M. and Prisecaru, I. (2009), Generic CANDU 6 plant severe accident analysis employing SCAPSIM/RELAP5 code, *Nuclear Engineering and Design*, pp 2093-2103.
[3] Mathew, P.M., Nitheanandan, T. and Bushby, S. J., *Severe Core Damage Accident Progression within a CANDU 6 Calandria Vessel*, *www.sar-net.org/upload/4-1_candu.pdf.*
[4] Luxat, D.L., and Luxat, J.C. (2007), Calandria Vessel Integrity under Severe Accident Loads, *Proceedings of SMiRT* 19.
[5] Dhir, V.K. (1998), Boiling Heat Transfer, *Annual Review of Fluid Mechanics*, pp 365-401
[6] Theofanous, T.G., Dinh, T.N., Tu, J.P., and Dinh, A.T. (2002), The boiling crisis phenomenon Part II: dryout dynamics and burnout, *Experimental Thermal and Fluid Science*, pp793-810.
[7] Theofanous, T.G., Syri, S., Salmassi, T., Kymalainen, O., Tuomisto, H. (1994), `Critical heat flux through curved, downward facing, thick walls`, Nuclear Engineering and Design, 151, 247-258.
[8] Yang, J., Dizon, M.B., Cheung, F.B., Rempe, J. L., Suh, K. Y. and Kim, S.B. (2005) `Critical Heat Flux for Downward Facing Boiling on a Coated Hemispherical Surface`, Experimental Heat Transfer, 18: 4, 223-242.

[9] Yang, S.H., Baek, W.P, Chang, S.H. (1997), Pool-boiling critical heat flux of water on small plates: effects of surface orientation and size, *International Communications in Heat and Mass Transfer*, pp 1093-1102.

[10] Guo, Z., El-Genk, M. (1992), An experimental study of saturated pool boiling from downward facing and inclined surfaces, *International Journal of Heat and Mass Transfer*, pp 2109-2117.

[11] Su. G.H., Wu, Y. W., and Sugiyama, K. (2008), Subcooled pool boiling of water on a downward-facing stainless steel disk in a gap, *International Journal of Multiphase Flow*, pp 1058-1066.

[12] Touloukian, Y. S., and C. Y. Ho, Eds. (1972), *Thermophysical Properties of Matter*, Vol. 1, *Thermal Conductivity of Metallic Solids*, Plenum Press, New York.